In conclusion, we have described a new and simple strategy for the molecular design of chiral phase-transfer catalysts by introducing a conformationally flexible, chiral $C_2$-symmetric quaternary ammonium bromide **4** and uncovering its characteristic feature. The representative phase-transfer alkylation of **2** was smoothly catalyzed by **4** in a highly enantioselective manner, which stems from the high chiral efficiency of a homochiral isomer rapidly equilibrating with a heterochiral one as verified by a variable-temperature $^1$H NMR study. Our approach conceptually parallels the successful utilization of a flexible ligand to magnify the effect of the other chiral ligand through a coordinative interaction with the metal center,[7] and should eventually offer a new dimension for asymmetric phase-transfer catalysis based on the design of the catalyst.

*Experimental Section*

Phase-transfer benzylation of **2** with catalyst **4d** (entry 6 in Table 1): Water (29.2 μL) was introduced to a 10-mL two-neck flask containing a Teflon-coated magnetic stirring bar and $CsOH \cdot H_2O$ (265 mg, 1.5 mmol) and the mixture was stirred under an argon atmosphere. Then, **4d** (5.8 mg, 0.005 mmol) and a solution of glycine *tert*-butyl ester benzophenone Schiff base **2** (148 mg, 0.5 mmol) in toluene (3 mL) were added and the mixture was cooled to $-15\,^\circ C$. After 10 min of gentle stirring, benzyl bromide (73.6 μL, 0.6 mmol) was added dropwise and the reaction mixture was stirred vigorously for 16 h. The resulting mixture was poured into brine (25 mL) and extracted with $CH_2Cl_2$ (6 mL × 3). The organic layer was dried over $Na_2SO_4$ and concentrated. The residual oil was purified by column chromatography on silica gel (diethyl ether/hexane = 1:20 to 1:10 as eluant) to give the corresponding benzylation product **3** (R = $CH_2Ph$) (168 mg, 0.436 mmol; 87 % yield, 94 % *ee*) as a colorless oil. The enantiomeric excess was determined by chiral HPLC analysis (Daicel Chiralcel OD, hexane/2-propanol = 100:1, flow rate = 0.5 mL min$^{-1}$, retention time; 13.7 min (*R*) and 24.6 min (*S*)).

Received: November 26, 2001
Revised: February 18, 2002 [Z18273]

[1] For reviews, see: a) M. J. O'Donnell in *Catalytic Asymmetric Synthesis* (Ed.: I. Ojima), Verlag Chemie, Weinheim, **1993**, chap. 8; b) T. Shioiri in *Handbook of Phase Transfer Catalysis* (Eds.: Y. Sasson, R. Neumann), Blackie Academic & Professional, London, **1997**, chap. 14; c) S. Ebrahim, M. Wills, *Tetrahedron Asymmetry* **1997**, *8*, 3163; d) "Phase-Transfer Catalysis": I. A. Esikova, T. S. Nahreini, M. J. O'Donnell, *ACS Symp. Ser.* **1997**, *659*, chap. 7; e) "Phase-Transfer Catalysis": T. Shioiri, A. Ando, M. Masui, T. Miura, T. Tatematsu, A. Bohsako, M. Higashiyama, C. Asakura, *ACS Symp. Ser.* **1997**, *659*, chap. 11; f) M. J. O'Donnell, *Aldrichimica Acta* **2001**, *34*, 3.

[2] For leading references, see a) M. J. O'Donnell, S. Wu, J. C. Huffman, *Tetrahedron* **1994**, *50*, 4507; b) E. J. Corey, F. Xu, M. C. Noe, *J. Am. Chem. Soc.* **1997**, *119*, 12414; c) S. Arai, Y. Shirai, T. Ishida, T. Shioiri, *Chem. Commun.* **1999**, 49; d) B. Lygo, J. Crosby, J. A. Peterson, *Tetrahedron Lett.* **1999**, *40*, 8671; e) F.-Y. Zhang, E. J. Corey, *Org. Lett.* **2000**, *2*, 1097; f) Y. N. Belokon, R. G. Davies, M. North, *Tetrahedron Lett.* **2000**, *41*, 7245.

[3] a) T. Ooi, M. Kameda, K. Maruoka, *J. Am. Chem. Soc.* **1999**, *121*, 6519; b) T. Ooi, M. Takeuchi, M. Kameda, K. Maruoka, *J. Am. Chem. Soc.* **2000**, *122*, 5228; c) T. Ooi, M. Kameda, H. Tannai, K. Maruoka, *Tetrahedron Lett.* **2000**, *41*, 8339; d) T. Ooi, M. Takeuchi, K. Maruoka, *Synthesis* **2001**, 1716.

[4] The catalyst **1** as well as the one with a 3,4,5-trifluorophenyl group at the 3,3′-position are going to be commercially available from Aldrich Chemical Co. Ltd. as (*S*,*S*)-β-naphthyl-NAS-bromide (**1**) [54,839-1] and (*S*,*S*)-3,4,5-trifluorophenyl-NAS-bromide [54,838-3].

[5] Recently, we addressed the intervention of rapid oxidation of the in situ generated enolates by molecular oxygen under aerobic conditions, and reported the advantage of anaerobic conditions to attain synthetically satisfactory chemical yields: T. Ooi, M. Takeuchi, D. Ohara, K. Maruoka, *Synlett* **2001**, 1185. Although the employment of anaerobic conditions requires longer reaction times, it generally provides a clean reaction and better results.

[6] The reactivity and selectivity differences between homo- and heterochiral metal complexes have been well documented, especially in the studies on nonlinear effects in asymmetric synthesis. For a recent excellent review, see: C. Girard, H. B. Kagan, *Angew. Chem.* **1998**, *110*, 3088; *Angew. Chem. Int. Ed.* **1998**, *37*, 2922.

[7] For impressive reports on the use of conformationally flexible ligands in transition metal catalyzed asymmetric synthesis, see: a) T. Hashihayata, Y. Ito, T. Katsuki, *Synlett* **1996**, 1079; b) T. Hashihayata, Y. Ito, T. Katsuki, *Tetrahedron* **1997**, *53*, 9541; c) K. Mikami, T. Korenaga, M. Terada, T. Ohkuma, T. Pham, R. Noyori, *Angew. Chem.* **1999**, *111*, 517; *Angew. Chem. Int. Ed.* **1999**, *38*, 495; d) K. Miura, T. Katsuki, *Synlett* **1999**, 783; e) J. Balsells, P. J. Walsh, *J. Am. Chem. Soc.* **2000**, *122*, 1802; f) M. D. Tudor, J. J. Becker, P. S. White, M. R. Gagne, *Organometallics* **2000**, *19*, 4376; g) T. Korenaga, K. Aikawa, M. Terada, S. Kawauchi, K. Mikami, *Adv. Synth. Catal.* **2001**, *343*, 284; h) K. Mikami, K. Aikawa, Y. Yusa, M. Hatano, *Org. Lett.* **2002**, *4*, 91; i) K. Mikami, K. Aikawa, Y. Yusa, *Org. Lett.* **2002**, *4*, 95; j) K. Mikami, K. Aikawa, *Org. Lett.* **2002**, *4*, 99.

[8] Although the benzylation of **2** with **4d** and aqueous CsOH at 0 °C proceeded faster to give **3** (R = $CH_2Ph$) in 84 % yield after 6 h, the enantioselectivity was found to be 83 % *ee* probably because of the background alkylation of the more nucleophilic cesium enolate. This observation led us to conduct the reaction at lower temperature, taking advantage of not only the simple temperature effect but also the increase of the existence ratio of homochiral isomer.

[9] a) Y. Fukazawa, S. Usui, K. Tanimoto, Y. Hirai, *J. Am. Chem. Soc.* **1994**, *116*, 8169; b) I. Azumaya, H. Kagechika, K. Yamaguchi, K. Shudo, *Tetrahedron* **1995**, *51*, 5277.

[10] The $^1$H NMR assignment of the homo- and heterochiral **4c** was conducted based on the $^1$H NMR spectra of conformationally rigid, diastereomeric **1** and **6**.

# A Model System Mimicking Glycosphingolipid Clusters to Quantify Carbohydrate Self-Interactions by Surface Plasmon Resonance**

María J. Hernáiz, Jesús M. de la Fuente, África G. Barrientos, and Soledad Penadés*

*Dedicated to Professor Julio D. Martin on the occasion of his 60th birthday*

Cell surface carbohydrates play a role in cell–cell adhesion and communication.[1, 2] Several models for cell interactions based on carbohydrates have been proposed. In most of them, the carbohydrate binds to selectins, galectins, and other

[*] Dr. S. Penadés, M. J. Hernáiz, J. M. de la Fuente, Á. G. Barrientos
Grupo de Carbohidratos
Instituto de Investigaciones Químicas, CSIC
Isla de La Cartuja, Américo Vespucio s/n, 41092 Sevilla (Spain)
Fax: (+34) 95-4460-565
E-mail: penades@cica.es

[**] This work was supported by the DGES (PB960820) and EC (HPMF-1999-00241). M.J.H. thanks the Marie Curie program for a grant. J.M.F. thanks the MEC for a predoctoral fellowship. We thank Dr. L. Kremer and the Department of Immunology and Oncology of CNB for biosensor facilities, and Prof. M. Martín-Lomas for helpful advice and fruitful discussions.

  1433-7851/02/4109-1554 $ 20.00+.50/0 

carbohydrate-binding proteins.[2] In 1989 Hakomori et al. proposed interactions between glycosphingolipid (GSL) microdomains as an initial step for adhesion and recognition.[3] The process would consist of a highly specific low-affinity $Ca^{2+}$-dependent multivalent interaction between the carbohydrate moieties at the cell surface.[4, 5] The antigen Lewis$^X$ ($Le^X$) is a trisaccharide (Gal$\beta$(1 $\rightarrow$4)[Fuc$\alpha$(1 $\rightarrow$3)]GlcNAc) carried by glycosphingolipids and poly-LacNAc ("embryoglycan"). Specific homotopic $Le^X$ – $Le^X$ interactions provide a possible basis for initial cell recognition in morula compaction and in embryonic carcinoma cells.[6, 7] Attempts to characterize and quantify this weak interaction in solution with monomeric $Le^X$ ligands have failed.[7, 8]

Recently, we have prepared gold nanoclusters functionalized with self-assembled monolayers (SAMs) of biologically significant oligosaccharides as a new water-soluble three-dimensional (3D) polyvalent model system mimicking GSL clusters.[9] With these gold glyconanoparticles we have demonstrated, by using transmission electron microscopy (TEM), the selective ability of the $Le^X$ determinant for self-recognition in calcium-containing aqueous solution.[9] This ability was also confirmed by an atomic force microscopy (AFM) study of adhesion forces between individual $Le^X$ antigen molecules by using well-defined 2D-SAM surfaces.[10]

Self-assembled monolayers of alkanethiolates on gold are structurally well-organized substrates that provide excellent model surfaces for studies in biology.[11, 12] At the same time surface plasmon resonance (SPR) has been developed as an analytical method to investigate molecular recognition in carbohydrate – protein binding in real time.[13] We now demonstrate that the combination of SAMs of alkanethiolates on gold presenting carbohydrate epitopes as the substrate, gold glyconanoparticles as the analyte, and detection by SPR constitutes an excellent approach for studying and quantifying, in a well-defined system, the putative $Ca^{2+}$-mediated carbohydrate-to-carbohydrate interactions. The results now reported: a) provide, for the first time, a quantitative estimation of the kinetics for the self-interaction of the biologically important $Le^X$ trisaccharide antigen; b) confirm the selective calcium dependency of this interaction; and c) illustrate, once more, the value of polyvalent presentation in the examination of weak interactions.[14]

Two important reports have been published recently on the quantitative estimation of carbohydrate interactions by SPR.[15, 16] In both of them the interacting oligosaccharides were attached to macromolecules (bovine serum albumin[15] or polymers[16]) that gave rise to a number of nonspecific interactions which hampered the study. In our system these unspecific interactions are minimized since the SAMs are prepared directly on the gold surface and we can control the nature of the ligand, its concentration, and its density at the gold surface.

The molecules used in this study are shown in Figure 1 A, and a schematic representation of a typical binding event (sensorgram) of our model system is given in Figure 1 B. $Le^X$ trisaccharide and lactose neoglycolipids **1** and **3** were synthesized with a linker terminating with a thiol group, which enables the preparation of both polyvalent gold glyconanoparticles of $Le^X$ (**1**-Au) and lactose (**3**-Au) as analytes and SAMs of **1** and **3** on the biosensor gold surfaces as substrates. The methyl glycosides **2** and **4** were also prepared as monovalent ligands.[17] Sensor chips functionalized with SAMs of 11-thio-3,6,9-trioxaundecanol (**5**) and 11-thioundecanol (**6**)

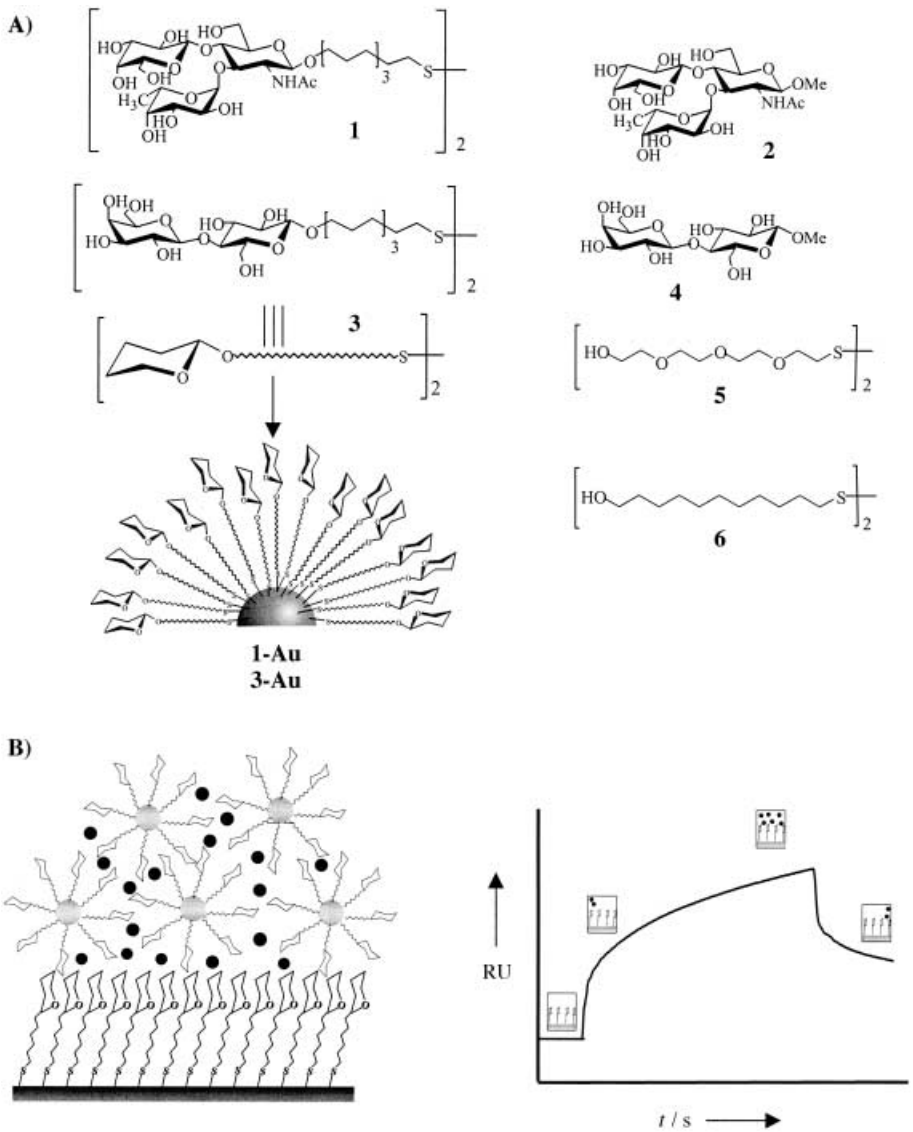


Figure 1. A) Structures of carbohydrate ligands used in this study; shaded hemisphere = gold nanoparticle. B) Schematic representation of our binding event strategy with a typical sensorgram; gray circles = gold nanoparticles, black circles = $Ca^{2+}$ ions.

  1433-7851/02/4109-1555 $ 20.00+.50/0 

were used as control surfaces. Glyconanoparticles **1**-Au and **3**-Au have been prepared and characterized previously.[9]

The SPR experiments were carried in a Biacore instrument (Biasensor AB, Uppsala) at 25 °C. A J1 biosensor chip (plain gold surface) was functionalized with neoglycolipids **1** (flow cell 1) and **3** (flow cell 2) at flow rate of 3 μL min$^{-1}$ until a constant SPR response (715 RU for **1** and 794 RU for **3**) was obtained (RU = response units). To cover possible gaps on the gold surface, the immobilization was continued by injection of an aqueous methanol solution (50 %) of **5** (2 mg mL$^{-1}$). In the third flow cell **5** was immobilized to remove any nonspecific interactions between the linker and carbohydrate ligands. The fourth flow cell of the sensor chip was treated only with buffer to serve as a second control. Alternatively, three different J1 sensor chips were functionalized by removing them from the plastic holder and soaking them in solutions of **1**, **3**, or **6** (2.5 mM) in ethanol. The results were similar to those obtained by the other protocol.

The binding of **1**-Au, **3**-Au, and the monovalent ligands **2** and **4** to SAMs of **1** and **3** were measured in Hepes buffer (Hepes = 2-[4-hydroxyethyl)piperazine-1-yl]ethanesulfonic acid) in the presence and absence of $Ca^{2+}$ ions.[18] Sensorgrams for the binding of **1**-Au, **3**-Au, and the corresponding monomeric ligands **2** and **4** to immobilized $Le^X$ and *lacto*-neoglycolipids are shown in Figure 2. A plot of $k_{obs}$ versus ligand concentration from the association phase yielded the rate constant $k_{on}$. At least six different concentrations of carbohydrate ligands were used. The dissociation rate constant $k_{off}$ was obtained from the direct analysis of the dissociation phase of the sensorgrams. The rate constants $k_{on}$ and $k_{off}$ and the apparent affinity constants $K_d$ are given in Table 1.

A slow association phase and a very gradual dissociation phase are shown in curves for the binding of $Le^X$ nanoparticles (**1**-Au) to $Le^X$ monolayers in the presence of calcium ions (Figure 2A). The binding is of high affinity, with a calculated $K_d$ of $5.4 \times 10^{-7}$ M (Table 1) and an RU value of 700 at a concentration of 1.8 μM. In contrast, binding of monovalent ligand **2** shows a very fast association and dissociation phase, which indicates a very weak interaction ($5.7 \times 10^{-3}$ M; Figure 2B). The ligands showed nonspecific interaction with the control lines (**5** and gold surface, data not shown). The data obtained suggest the importance of multivalent presentation of the ligand and how this contributes significantly to the binding affinity. No binding was observed in the absence of calcium ions. In comparison to the studies with $Le^X$ glyconanoparticles, the binding of *lacto*-glyconanoparticles (**3**-Au) to lactose monolayers exhibits a rapid association phase but a slightly lower response (275 RU) and a very fast dissociation phase (Figure 2C). The $K_d$ drops to $1.5 \times 10^{-5}$ M which indicates that the affinity and strength of the binding decrease to the mM range for the lactose – lactose interaction (Table 1). No binding was observed for the monomeric ligand **4** either in the presence or absence of $Ca^{2+}$ ions.

Table 1. Kinetic data ($k_{on}$, $k_{off}$, and $K_d$) and energy of binding ($\Delta G$) for monovalent and polyvalent ligands at 25 °C.[a]

| Monolayer surface | Carbohydrate ligand | $k_{on}$ [M$^{-1}$s$^{-1}$][b] | $k_{off}$ [s$^{-1}$][b] | $K_d$ [M][b] | $-\Delta G$ [kcal mol$^{-1}$] |
|---|---|---|---|---|---|
| **1** | **1**-Au | $2.8 \times 10^3$ | $1.5 \times 10^{-3}$ | $5.4 \times 10^{-7}$ | 8.5 |
| **1** | **2** | $7.0 \times 10$ | 0.4 | $5.7 \times 10^{-3}$ | 3.0 |
| **1** | **3**-Au | $5.0 \times 10^2$ | 0.4 | $80 \times 10^{-3}$ | 4.2 |
| **1** | **4** | –[c] | –[c] | –[c] | –[c] |
| **3** | **3**-Au | $1.7 \times 10^3$ | $2.4 \times 10^{-2}$ | $150 \times 10^{-3}$ | 6.5 |
| **3** | **4** | –[c] | –[c] | –[c] | –[c] |
| **3** | **1**-Au | $1.0 \times 10^2$ | $1.0 \times 10^{-2}$ | $10 \times 10^{-3}$ | 5.4 |
| **3** | **2** | –[c] | –[c] | –[c] | –[c] |

[a] 10 mM Hepes buffer (pH 7.4), 150 mM NaCl, 10 mM $CaCl_2$. The size of the statistical parameter $\chi^2$ is $< 3$ in all the fitting curves. [b] On the basis of the glyconanoparticle concentration. [c] After substracting the data for nonspecific interactions from the gold and **5** surfaces (control lines) the signal was below 10 RU.

Crossed SPR experiments between immobilized Lewis X and *lacto*-nanoparticles or vice versa also gave affinity constants in the mM range (Table 1). Monovalent ligands **2** and **4** did not show any interaction in the crossed experiments. Similarly, the response observed for the interaction of the poly- (**1**-Au, **3**-Au) and monovalent (**2** and **4**) ligands with the immobilized monolayers of **5** and **6**, after subtracting background binding to the gold surface, was below the detection sensibility of the signal in the Biacore instrument (RU < 10). Thus, no selective interaction occurs between carbohydrate ligands and these surfaces.

These results indicate that the affinity of the $Le^X$ antigen for self-recognition is in the μM range, whereas the lactose self-interaction and the heterotopic $Le^X$ – *lacto* interaction show affinity constants in the mM range. The selectivity of $Le^X$ nanoparticles for the $Le^X$ monolayer is about 200 times higher ($\Delta\Delta G \sim 3$ kcal mol$^{-1}$) than for the *lacto* monolayer and 30 times higher ($\Delta\Delta G \sim 2$ kcal mol$^{-1}$) than that of the *lacto* nanoparticles for its self-assembled monolayers (Table 1). The binding affinity for $Le^X$ self-recognition ($\Delta G \sim 8$ kcal mol$^{-1}$) equals the

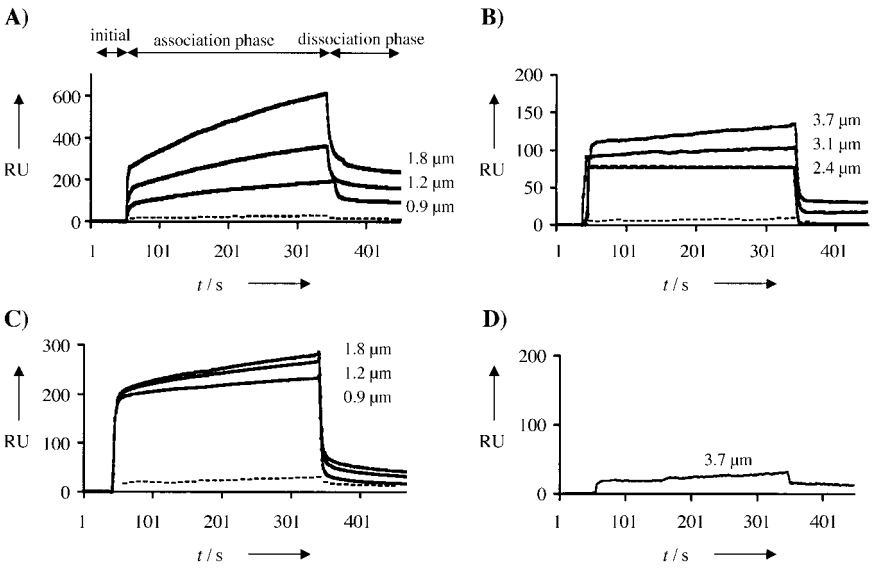


Figure 2. SPR sensorgrams for the interaction of: A) **1**-Au to SAMs of **1**; B) **2** to SAMs of **1**; C) **3**-Au to SAMs of **3**; D) **4** to SAMs of **3**, without (- - - -) and with $Ca^{2+}$ ions (——).

  1433-7851/02/4109-1556 $ 20.00+.50/0 *Angew. Chem. Int. Ed.* **2002**, *41*, No. 9

affinity determined for the heterotopic binding of polymeric Gg3 to GM3 monolayers,[16] which is a model system mimicking the Gg3–GM3 interaction between lymphoma and melanoma cells.[19] However, the selectivity found for the $Ca^{2+}$-mediated $Le^X$–$Le^X$ interaction related to the $Le^X$–*lacto* in our model system is about 3 kcal mol$^{-1}$ higher than that found between Gg3–GM3 and Gg3–*lacto* interactions ($\Delta\Delta G <$ 1 kcal mol$^{-1}$) in the monolayer–polymer system.[16]

The selective $Le^X$–$Le^X$ recognition in our model system is $Ca^{2+}$ dependent. In the absence of $Ca^{2+}$ ions, $Le^X$ nanoparticles bind to all functionalized surfaces as they do to the bare gold surface (Figure 2A). The selective role of $Ca^{2+}$ ions is also shown in the apparent rate of dissociation of $Le^X$ nanoparticles–$Le^X$ surface complex (Figure 2A). Addition of 10 mM ethylenediamine tetraacetate (EDTA) solution to the buffer was necessary to remove the $Le^X$ surface associate complex, whereas in the case of the *lacto*–*lacto* complex, buffer solution was sufficient to regenerate the *lacto*-functionalized surface (Figure 2C). These and our previous results from transmission electron microscopy (TEM)[9] indicate that $Ca^{2+}$ ions are necessary for selective $Le^X$ self-recognition and agree also with the early observation of $Ca^{2+}$-dependent aggregation of $Le^X$-coated beads.[7] In contrast, the presence of calcium ions does not contribute significantly to the adhesion forces in the atomic force microscopy (AFM) experiment.[10] This selective calcium dependency may also explain the differences in binding behavior between the monomeric ligands $Le^X$ **2** ($K_d = 5.7$ mM) and lactoside **4** (Figure 2B and D). The response observed for **2** (130 RU), despite its low molecular weight, may be due to $Ca^{2+}$-mediated higher molecular aggregates that allow the detection of the interaction on the SPR experiment. This may be also the reason that the apparent affinity of monomeric $Le^X$ (**2**) for immobilized $Le^X$ monolayers, as measured by SPR, is two orders of magnitude higher than that obtained for the binding of **2** to $Le^X$-containing liposomes ($K_d = 0.3$ M), as determined by NMR spectroscopy.[20]

The elusive nature of carbohydrate–carbohydrate interactions, which has made their identification and study very difficult, has been our focus since 1990.[21] We provide here the first quantitative kinetic data for $Le^X$ self-recognition and direct evidence of its $Ca^{2+}$ dependency. The cooperative character of this polyvalent interaction has been proved as well ($\beta = 10^4$).[14] Low multivalency may be the reason that $Le^X$ self-recognition could not be observed in other model systems.[15] In addition, incorrect presentation of the oligosaccharide epitopes may be responsible for the weak interaction observed in liposome systems.[20, 22] The data here reported, together with our previous results,[9] clearly support the proposal that $Le^X$ carbohydrate self-interaction can be a relevant mechanism for cell adhesion and recognition.[6] Gold glyconanoparticles and SAMs presenting carbohydrate epitopes constitute an excellent biomimetic model of carbohydrate presentation at the cell surface. These tools together with the application of new analytical techniques (SPR and AFM) are allowing us to unravel the molecular basis of other carbohydrate-mediated interactions.

Received: December 6, 2001 [Z18337]


[1] a) S.-i. Hakomori, *Cancer Res.* **1996**, *56*, 5309–5318; b) S.-i. Hakomori, *Glycoconjugate J.* **2000**, *17*, 627–647.

[2] a) W. I. Weis, K. Drickamer, *Annu. Rev. Biochem.* **1996**, *65*, 441–473; b) Y. C. Lee, R. T. Lee, *Acc. Chem. Res.* **1995**, *28*, 321–327.

[3] I. Eggens, B. A. Fenderson, T. Toyokuni, B. Dean, M. R. Stroud, S.-i. Hakomori, *J. Biol. Chem.* **1989**, *264*, 9476–9484.

[4] D. Spillmann, M. M. Burger in *Carbohydrates in Chemistry and Biology, Vol. 2* (Ed.: B. Ernst, G. W. Hart, P. Sinaÿ), Wiley-VCH, Weinheim, **2000**, pp. 1061–1091.

[5] J. Rojo, J. C. Morales, S. Penadés, *Top. Curr. Chem.* **2002**, *218*, 45–92.

[6] S.-i. Hakomori, *Pure Appl. Chem.* **1991**, *63*, 473–482.

[7] N. Kojima, B. A. Fenderson, M. R. Stroud, R. I. Goldberg, R. Habermann, T. Toyokuni, S.-i. Hakomori, *Glycoconjugate J.* **1994**, *11*, 238–248.

[8] M. R. Wormald, C. J. Edge, R. A. Dwek, *Biochem. Biophys. Res. Commun.* **1991**, *180*, 1214–1221.

[9] J. M. de la Fuente, A. G. Barrientos, T. C. Rojas, J. Rojo, J. Cañada, A. Fernández, S. Penadés, *Angew. Chem.* **2001**, *113*, 2318–2321; *Angew. Chem. Int. Ed.* **2001**, *40*, 2258–2261.

[10] C. Tromas, J. Rojo, J. M. de la Fuente, A. G. Barrientos, R. García, S. Penadés, *Angew. Chem.* **2001**, *113*, 3142–3145; *Angew. Chem. Int. Ed.* **2001**, *40*, 3052–3055.

[11] M. Mrksich, G. M. Whitesides, *Annu. Rev. Biophys. Biomol. Struct.* **1996**, *25*, 55–78.

[12] M. Mrksich, *Chem. Soc. Rev.* **2000**, *29*, 267–273.

[13] S. R. Haseley, J. P. Kamerling, J. F. G. Vliegenthart, *Top. Curr. Chem.* **2002**, *218*, 94–114.

[14] a) M. Mammen, S.-K. Choi, G. M. Whitesides, *Angew. Chem.* **1998**, *110*, 2908–2953; *Angew. Chem. Int. Ed.* **1998**, *37*, 2754–2794.

[15] S. R. Haseley, H. J. Vermeer, J. P. Kamerling, J. F. G. Vliegenthart, *Proc. Natl. Sci. USA* **2001**, *96*, 9419–9424.

[16] K. Matsuura, H. Kitakouji, N. Sawada, H. Ishida, M. Kiso, K. Kitajima, K. Kobajashi, *J. Am. Chem. Soc.* **2000**, *122*, 7406–7407.

[17] A. G. Barrientos, J. M. de la Fuente, T. C. Rojas, A. Fernández, S. Penadés, unpublished results.

[18] In a typical experiment, a 15-μL injection of ligand at different concentrations (3.7, 3.1, 2.4, 2.0, 1.5, 1.0 mM for the monovalent ligand and 1.8, 1.2, 0.9, 0.4, 0.1 μM for the polyvalent ligand) in Hepes (10 mM, pH 7.4, 150 mM NaCl without or with 10 mM $CaCl_2$) buffered saline was made at a flow rate of 3 μL min$^{-1}$. At the end of each sample injection, the sensor surface was washed continuously with buffer solution to allow dissociation. After a suitable dissociation phase the sensor surfaces were regenerated for the next ligand sample by three sequential injections (10 μL of 10 mM EDTA solution, 70% methanol in water, and Hepes-buffered saline). The response was monitored as a function of time (sensorgram) at 25 °C. Data from the control cells were used to estimate the contribution of nonspecific interactions with the gold and chain surface. Kinetic parameters were determined by using the Biacore BIAevaluation software from Biacore (Version 3.0.2, 1999).

[19] K. Iwabuchi, S. Yamamura, A. Prinetti, K. Handa, S.-i. Hakomori, *J. Biol. Chem.* **1998**, *273*, 9130–9138.

[20] A. Geyer, C. Gege, R. R. Schmidt, *Angew. Chem.* **1999**, *111*, 1569–1571; *Angew. Chem. Int. Ed.* **1999**, *38*, 1466–1468.

[21] a) J. M. Coterón, C. Vicent, C. Bosso, S. Penadés, *J. Am. Chem. Soc.* ***1993***, *115*, 10066–10076; b) J. Jiménez-Barbero, E. Junquera, M. Martín-Pastor, S. Sharma, C. Vicent, S. Penadés, *J. Am. Chem. Soc.* **1995**, *117*, 11198–11204; c) J. C. Morales, D. Zurita, S. Penadés, *J. Org. Chem.* **1998**, *63*, 9212–9222.

[22] F. Pincet, T. Le Bouar, Y. Zhang, J. Esnault, J.-M. Mallet, E. Perez, P. Sinaÿ, *Biophys. J.* **2001**, *80*, 1354–1358.


  1433-7851/02/4109-1557 $ 20.00+.50/0 